# Design for the environment: HJT module with ultra-low carbon footprint

Timea Bejat, Nouha Gazbour, Amandine Boulanger, Rémi Monna, Renaud Varache, Jérôme Francois, Wilfried Favre, Charles Roux, Aude Derrier, Eszter Voroshazi

# DESIGN FOR THE ENVIRONMENT: SHJ MODULE WITH ULTRA-LOW CARBON FOOTPRINT

Timea Béjat[1], Nouha Gazbour[1], Amandine Boulanger[1], Rémi Monna[1], Renaud Varache[1], Jérôme François [2], Wilfried Favre[1], Charles Roux[1], Aude Derrier[1], Eszter Voroshazi[1]
[1]Univ. Grenoble Alpes, CEA, LITEN, INES, 73375 Le Bourget du Lac, France
[2]Univ. Grenoble Alpes, CEA, LITEN, INES, ITE INES.2S, 73375 Le Bourget du Lac, France
timea.bejat@cea.fr,

**Abstract:**

The photovoltaic (PV) industry is reaching an inflection point to become a major source of energy. Reducing its environmental impact is means of product differentiation but the foremost it is a cornerstone to maintain a sustainable growth of the sector, and to meet societal challenges. Committed to this approach for several years, our paper presents the development of heterojunction modules (SHJ) with exemplary power and reliability with significantly reduced environmental impact and components sourced from Europe. In order to guide the technology choice in the design phase, we performed a Life Cycle Assessment (LCA) sensitivity study. This led us to act on the most critical lines of the carbon footprint reduction, namely the silicon wafers, the origin of the components, the glass front panel and the aluminium frame. At the cell scale, we achieved the reduction of the carbon footprint by reducing the thickness of the wafers issued from the European value chain. Optimization of metallization and cell interconnection has limited the consumption of silver, a critical raw metal. At the module level, we implemented the reduction of glass thickness and the replacement of the aluminium frame with a natural fibre based frame in a glass-backsheet module configuration. In addition, we applied a "design for recycling" approach for the choice of encapsulant and backsheet. The combination of these innovations led us to the realization of a 566 Wp recyclable module using a paving interconnection, cells with an average efficiency of 22.9 % with a carbon footprint of 317 $kgCO_2eq/kWp$.

Keywords: gapless interconnection, SHJ, low carbon footprint, timber frame, LCA

Highlights:

- Presenting a design for the environmental approach from conception to realization of industrial-scale prototype with the technical challenges of combining multiple technical and material innovations.
- Combination of SHJ cell on thin wafers < 120 µm with reduced Ag, In content has been implemented on low carbon wafers sourced in the EU.
- Paving interconnection using electrically conductive adhesive (ECA) based on low temperature and Pb-free interconnection technology, with reduced Ag content.
- Case study of low carbon frame: implementation of natural fiber (timber) frame and its initial reliability study is novelty in the field.
- On module level, the bill-of-materials (BOM) selection with design for recycle motivated the choice of thermoplastic encapsulant, fluorine and Al-free backsheet and thin front glass.

# 1 Introduction

The cumulative deployment of photovoltaics in 2022 has reached the Terawatt scale worldwide, and exponential growth is underway [1]. The PV industry is reaching an inflection point to become one of the major sources of energy, even dominant in some regions. Optimizing the environmental impact of this technology is becoming a leverage for industrial competitiveness and maintaining the growth of the sector as well as addressing societal issues. National and European legislations as well as industrial alliances strongly support the implementation of an eco-design approach. Several environmental initiatives have been launched in the PV sector to improve the environmental profile of PV systems. At European level, a new eco-design label of PV with a threshold of the carbon footprint had been launched [2]. At the national level, the French Energy Regulator (CRE) had fixed a carbon footprint threshold about 550 kg$CO_2$eq. / kWp for the next national call of tender [3]. Similarly, the Ultra-Low Carbon Solar (ULCS) Criteria has been set by USA, with funding from the Ultra Low-Carbon Solar Alliance (ULCSA) and Global Electronics Council (GEC). The embodied carbon of the PV module shall be equal to or less than 630 kg $CO_2$eq. / kWp [4]. Therefore, manufacturers have stepped up their efforts to meet these regulations requirements and penetrate the market. Low-carbon photovoltaic panels are beginning to be proposed by pioneering manufacturers (without an exhaustive list naming REC, Bisol, Qcells, Voltec etc.)[5] [6] [7]. The carbon footprint is currently the reference criterion used by the industry and by the public authorities. Nevertheless adopting an eco-design approach means reducing the product's environmental footprint broadly by lowering its impact on the entire life cycle (use stage, end of life stage…) and on all environmental criteria such as the resources' use [8].

Committed to this approach for several years at CEA-INES, the objective of this study is the development of silicon heterojunction modules (SHJ) with a significant environmental impact reduction and component sourcing locally for resilience. We follow an eco-design approach from conception stage to optimize jointly cell, interconnection and bill-of-materials (BOM), and thus lowering the critical resources' use and anticipating the recycling of the PV module for a low environmental impact.

The Life Cycle Assessment (LCA) methodology is known as the most powerful and reliable tool to assess the environmental profile of a product [9]. It is a standardized assessment method (ISO 14040 [10] [11] and ISO 14044 [12]) which allows the evaluation of the potential environmental impacts of products throughout their life cycle and was used for this study to guide the technological choice from the early design process [13]. PV module manufacturing covers a chain of separate successive actions that can be optimised separately to reach an exemplary level of environmental impact, considering each part of the value chain as giving a final product [14]. The first separate *final product* is SHJ solar cell. The SHJ cells are made of a crystalline silicon wafer, coated by electro-active layers during cell manufacturing. This silicon wafer has the highest environmental impact within the PV module structure [15] as during its manufacturing large amount of energy is necessary to purify silicon ingots. Several studies had focused on actions to reduce wafers environmental impact while maintaining cells electrical performance such as reducing its thickness [16] [17]. The selected solar cells then must be integrated in PV module for that we need to choose the lowest environmental impact bill-of-materials (BOM) and module configuration. Müller et al. [18] suggested that GBS configuration may have a worse environmental impact than GG configuration in case of high hard coal share within the country's energy mix as it is the case for China. Thus they compared G/BS configuration with components from China with G/G configuration with components from Germany and then from the EU. According to energy mix data, the environmental impact assessment showed worst total results for G/BS module with hard coal energy mix country (in that case Chine) compared to other example.

In the following, we targeted glass/backsheet (GBS) configuration instead of glass/glass (GG) one produced in the European Union (EU). Standard PV module structure contains a glass front sheet, encapsulant at the front and rear side of the interconnected cells as adhesive to attach the module structure together and back sheet acting as rear cover. To act on each line in the material balance, we analysed the environmental impact/energy performance/price couple of available materials. The main criteria for front sheet materials is the highest light transmission rate and the mechanical protection. Solar grade and tempered glass is still the reference material for standard c-Si PV panels thanks to their abundance (low price) and its proven reliability, despite the emergence of new polymer materials on the market with higher light transmission rates and considerably lower weight, for example, ethylene tetra fluoro ethylene (ETFE) materials [19] [20]. Solar glass dedicated to PV modules belongs to two main categories: soda lime glasses and borosilicate glasses [21] and are among the most impacting components of a PV module in the LCA balance. Similar to silicon wafers, the first action to consider is thickness reduction. Allsopp *et al.* [22] showed the improvements in glass composition which may lead to improved PV module performance, such as low iron content and use of anti-reflective coating (ARC) to emphasise light transmittance. Thanks to the recent increase of solar glass prices, the market availability of thin solar glasses had exploded. Several suppliers propose up to 1.8 mm thick glasses for large area solar module manufacturing, up to 2.9 m² sized modules. This progression has an unwilled aspect large area glasses require careful and specially adapted handling during assembly process.

Solar grade polymer encapsulants can be divided into to two mains categories: chemically non-crosslinking and chemically cross-linking ones [23]. The cross-linking reaction of polymer encapsulants consists in the formulation of secondary links between primary polymer chains. Curing agents, peroxides, added to the polymer during its manufacturing, catalyse this reaction to ensure the encapsulant's thermo-mechanical stability. The reaction starts at predefined boundary conditions usually at a given temperature that meet the material during lamination. The question of recycling after cross-linking needs to be addressed as traditionally these encapsulants are subject to grind or incineration during recycling instead of chemical or mechanical separation of PV module layers. Chemically non-crosslinking encapsulant families are thermoplastic elastomers (TPO), ionomers and poly vinyl butyrals (PVB). PVB are less used today as their high water uptake is disadvantageous compared to other encapsulants. Ionomers present good water ingress resistance but lower adhesion and a tough mechanical behaviour. They were identified as candidate encapsulants for new generation PV modules (perovskites and tandems), but their mechanical performance suggest to discard them from those applications and orient their use more toward to integrated PV solutions [24]. TPOs are promising candidates for low environmental impact PV applications [25] as they are exempt of harmful by-product generation during degradation contrary to EVA [26], [27]. Their non-cross-linked nature facilitates recycling at PV module's end of life (EoL). Nevertheless Jia *et al.* [17] pointed out that TPO encapculants are a good choice to lower LCA balance and Segbefia *et al.* listed the advantages and inconveniences of main encapsulant families with TPOs [28]. It is important to recall that all non-crosslinkeable encapsulants have less than 2 % of market share today.

Market leader backsheets contain fluoro-polymers. Polyvinyl fluoride (PVF) and Polyvinylidene fluoride (PVDF) share 80 % of the market and the most popular actual backsheets are coated BS on both sides. The main disadvantage of fluorine containing backsheets is the harmful by-products generation at their EoL and during actual recycling processes [29]. To avoid this already identified problem polyethylene terephthalate (PET) based multilayer backsheets without fluorine content are emerging on the market.

Interconnection critical raw materials, and implementation of reduction, recycling and re-use are essential to ensure availability and price stability [30], [31]. Valero at el. [32] had pointed out the possible risks linked to raw material use of, among others, solar technology. Silver and indium are the most commonly cited as they may exceed the available resources with increasing demand by 2050. Hallam et al. [31] showed the criticality of silver in PV applications towards terawatt deployment as all actual PV cell technology are dependent of its availability. These projections are technology dependent and contain a large uncertainty therefore Zhang et al. [30] suggested depletion scenarios in function of PV cell technologies spread in the future. Typically, for silver a drastical reduction is required if terawatt scale is expected for 2050. Today's actions are focused on reduction of these elements in current PV technologies [33], [34] [35] with special attention dedicated to PV related materials' recycling process and technologies.

PV module framing is a standard process to straighten the structure to enable its integration on racks or on vertical surfaces. Traditional frame material is aluminium but as environmental impact of this material is important compared to other construction materials, new stressors enter on market such as steel [36], [37], [38], plastic [39] or bio based materials to propose more ecologic solutions. These laters are still trials, as their application remains marginal. Steel enables lower environmental impact and increase tear-resistance of the PV module frame. Nevertheless its mechanical transformation requires heavier machines to obtain a final product suitable form PV framing due to stiffness of the material compared to aluminium. Aluminium frames are still subject of optimisation. Tummalieh et al. [40] presented a holistic design improvement giving a numerical simulation (finite element method) helped way to optimise frame structure. They found that decreasing frame section allows cell stress reduction while keeping life cycle impact low. Nevertheless they highlighted the holistic character of the optimisation, only mechanical optimisation will lead to economically unliveable solutions or to too high environmental impact. All parameters interact and may be considered simultaneously. Wood frames have few examples in installed structures. Singer [41] set up a complete study including conception and LCA and LCCA. As he pointed out, the most crucial phase of the conception is the frame section optimisation, which enables to obtain a sufficient mechanical strength by keeping low the material use and then the coast. That study remains at a manual level; no industrial lookout was involved in the process. Hossain et al. [42] showed a prototype with a wooden frame integrated to road surface, without up-scaling recommendations.

Wood frames have few examples in installed structures. Singer [41] set up a complete study including conception and LCA and LCCA. As he pointed out, the most crucial phase of the conception is the frame section optimisation, which enables to obtain a sufficient mechanical strength by keeping low the material use and then the cost. That study remains at a manual level; no industrial lookout was involved in the process. Hossain et al. [42] showed a prototype with a wooden frame integrated to road surface, without up-scaling recommendations.

Usually wood is associated to PV rack structure without mentioning framing. Often as a simple truss serving as a support,[43] and less currently to bring new functionalities to the module such as mobility [44] as a part of adaptive facades' structure. Classical façade integration of PV (BIPV systems) often has wood-based parts such as the example developed by Farkas et. [45] These latter studies promise a rich architectural potential of this material.

# 2 Materials and methods

## 2.1 LCA analysis

Eco-design is defined by the International Organisation for Standardisation (ISO 14006, 2011) [8] as "*the integration of environmental aspects into the design and development of products, with the aim of reducing negative environmental impacts throughout the life cycle of a product*". Therefore, the eco-design is an approach that reduces the negative impacts of the product throughout its life cycle, while maintaining its quality of use (cost, technical performance, etc.). Adopting an eco-design approach consists in three steps according to Vallat el al. [46]:

- Environmental assessment of the reference product
- Suggest eco-design strategies to reduce the environmental impacts in the development of the new solution;
- Prototype development according to previously defined strategy.

Following these steps, we define the LCA of a reference product as a first step. It enables to identify the hotspot in the value chain and guide technological choice to develop an eco-designed PV module. LCA is based on four main phases: (a) goal and scope, (b) inventory analysis, (c) impact assessment and (d) interpretation. The objective of this analysis is to compare both reference and developed product's environmental assessment. For this, we used EF3.0 method implemented in SimaPro 9.3 software. We used Ecoinvent 3.8 database completed by in-house data gathered by our team. Table 1 lists the considered environmental impact categories involved in this analysis.

| Eco-system | Human health | Earth damage | Resource depletion |
|---|---|---|---|
| Climate change | Ionising radiation | Acidification | Resource use, fossils |
| Ozone depletion | Particulate matter | Eutrophication, freshwater | Resource use, minerals and metals |
| Photochemical ozone formation | Human toxicity, non-cancer | Eutrophication, marine | |
| | Human toxicity, cancer | Eutrophication, terrestrial | |
| | | Ecotoxicity, freshwater | |
| | | Water use | |

*Table 1 List of environmental impact categories*

## 2.2 HJT Solar cells processing and characterization

For the present study CEA pilot line produced M2 SHJ rear junction cells of approximatively 130 µm thickness with 0.9–1.3Ω cm resistivity were used. As for a previous study [47], M2 n-type Czochralski wafers' surfaces were textured with an alkaline solution to form randomly distributed pyramids (3–7 µm), and then cleaned with ozone/hydrofluoric acid-based chemical process with anoxide removal as a final step. To complete the cell's structure, we used RF-PECVD technique to deposit on both sides doped a-Si:H and intrinsic layers and then n-type on front and p-type doped s-Si:H layer on the rear side. To complete the structure TCO layers were added on each side. Finally, silver paste was deposited by screen-printing using a 6 busbar design on both sides and cured at 200 °C during 15 min. We used

non-symmetrical structure, 1.5 mm pitch on the front and 0.7 mm on the rear side. Cell bifaciality factor remained in the range of 92%. For more details one can refer to [48], [49], [50] [47].
Solar cells were I-V characterized with a sun simulator to obtain efficiency (η), short circuit current density (Jsc), open circuit voltage (Voc), fill factor (FF), series resistance and shunt resistance by fitting the data points to the two-diode model for a solar cell. Measurements were performed with front side illumination, black chuck, and no rear illumination, using busbar contacts for both sides [51].

## 2.3 Module fabrication and process qualification

We focused on two different module sizes: mini-modules of 710*674 mm² area for material level testing and 2166x1297 (2.81 m²) full size modules for final proof of concept. The mini-modules had four strings of eight half-cut M2 cells in series connection, while for the final demonstrator 16 strings of 13 half-cut M2 cells are connected in butterfly configuration with 3 central diodes.

With the selected cells, at mini-module scale strings of 8 half-cut HJT M2 cells are fabricated with Ag ribbon gluing with ECA with a previously qualified process [52]. For the final modules 13 half-cut SHJ M2 cells are assembled in strings. The peel test has been used to qualify the adhesion of interconnect ribbons to solar cell metallization. Peel tests were carried out using a motorized tensile tester with a speed of 50 mm/min and a peel angle of 90°. Measured peel forces and fracture patterns are used as quality criteria to accept or reject a string of cells for integration into a module, to validate a new metallization paste formulation or a conductive adhesive, and to adjust manufacturing processes.

Glass-Backsheet mini-modules are manufactured using thermoplastic olefin (TPO) encapsulant rather than the standard ethylene vinyl acetate (EVA). Between these two sizes, a lamination process upscaling was necessary. With this specific adaptation, we can avoid laminations defects (e.g.bubble creation, displacement of cell-strings or cell cracks). We used a hot vacuum double plate laminator with a cooling unit. An optimisation process (temperature, pressure) preceded the final module assembly, to reach optimal adhesion between encapsulant and glass, backsheet, as well as a homogenous encapsulant layer without any damage to cells. We validate the lamination process with DSC and adhesion testing to control the adhesion at the glass/encapsulant and encapsulant/backsheet interfaces in 180° configuration.

## 2.4 PV module initial performance characterisation and accelerated ageing

The I-V measurements are conducted at room temperature (21 – 24 °C) on a A+A+A+ flash tester with a flash duration of 250 ms. A temperature correction is done to obtain the measurements at 25 °C. The I-V results are obtained for standard test conditions (1000 W/m², AM1.5G and 25 °C).
Electroluminescence imaging (EL) is captured with a GreatEyes CCD Silicium cam-era at 1 sun equivalent current injection. Samples are measured at their initial stage and at regular intervals during ageing test for both types of measurement.

Accelerated aging was conducted in damp heat and UV/TC/HF conditions according to [53] in mini module configuration. The reference module used for this study during the accelerated aging had exactly the same BOM as the test modules, except the cell interconnection, where we applied a 2 mm inter-cell gap during stringing process.

## 2.5 Module material qualification

First phase of BOM qualification serves to fix lamination parameters such as raw material dimensions or process temperature. To determine the raw material dimensions before their module integration, we measure withdrawal rate in both, machine and cross directions. It helps to avoid lack of material due to thermal withdrawal during lamination. As a second step, we used a differential scanning calorimetry (DSC) instrument, (TA Waters Q20 model), for among others, melting temperature definition. The apparatus uses a reference empty capsule, and a sample-filled one to analyze the difference between heat fluxes across each capsule's bottom surface. To prepare the launch of this analysis, we used aluminium hermetic pans and lids, closed by a crimper supplied by the machine manufacturer. The samples weighed between three and six milligrams and all measurements were carried out under a continuous nitrogen flow to prevent oxidation. The DSC measurement procedure involved three steps. First, a heating scan from 40 °C to 100 °C at a thermal rate of 10 °C/min was performed to eliminate the thermal history of our samples. Subsequently, a cooling step from 100 °C to -20 °C was achieved at the same rate to reveal the recrystallization region. Finally, a second heating scan from -20 °C to 250 °C was executed at 10 °C/min to observe both the melting and the curing agent decomposition regions. DSC analysis enables to calculate the crosslinking rate of a laminated solar encapsulant according to IEC62788 [54] standard. In the following we carried out peeling tests at initial and at two intermediate stages (after 500h and 1000h of DH exposure) on laminated samples (20 cm*20 cm) without solar cells to test bending between the selected encapsulant and backsheet. Peeling was realised according to IEC 61215-1 [53] standard at 180 ° configuration on two samples and three stripes/exposure time on each. We used an Instron 3365 machine with a special accessory for this standardised test which is available from the machine supplier and requires rigid support to attach to the base of the fix part of the device (in our case the front glass).

For the module validation, we manufactured one module with testing configuration and one as a reference. In both the same BOM and solar cells were used with only difference in interconnection: reference module had intercell of 2 mm while testing module had paving interconnection with overlapping cells. For aging sequences, we used 4x8 ½ cells modules (710mmx674mm).

## 2.6 Mechanical testing of modules with timber frame

First frame material test concerns wood four point bending test. It aims to preselect candidate wood species for further integration into full size PV modules. To carry out these tests, samples of developed section of 60 cm length were tested on an Instron 3365 device with special 4 point bending accessory [55] according to ASTM D6272 standard [56]. The loading was static flexure up to the machine limit (in our case 5000N) or until rupture.

Once the frame cross section geometry fixed, we carried out static mechanical load (SML) and dynamic mechanical load (DML) tests on module integrated timber frames. For these tests, classic modules were used (144 ½ M2 cells), Glass/Glass configuration to focus on frame performance and avoid new BOM interference on results. All tests followed the standards IEC61215 – MQT16 [53] for SML and IEC 62782 [57] for DML.

# 3 RESULTS AND DISCUSSION

## 3.1 LCA sensitivity analysis

As the main objective of the study is to develop an eco-designed PV module from the early design process the system boundary is limited to the manufacturing stage of the PV module (cradle to gate) from the extraction of the silicon to the assembly of the cells in a PV module. The functional unit used to express the environmental impacts is the "1 kWp of a PV module". In order to define the performance of the PV module of reference a benchmark of the market trends throughout the value chain was conducted. The Siemens process is the most widely used to produce the polysilicon covering more than 85% of world production [58]. This process produces very high quality silicon, but is considered to be very energy-intensive [59] which could impact the carbon footprint of the PV module specially with Chinese electricity mix [60]. Once the silicon has been purified, it is converted into solid form by the crystallization process, with the aim of increasing yield while preserving the quality of the material: this is the ingot (c-Si). Due to its high quality and low cost these last years, monocrystalline ingots dominate the market with more than 95 % of market share in 2022 [58]. The polycrystalline silicon represented less than 5 % in 2022 and is likely to disappear from the market by 2025 [58]. Nevertheless, the standard Czochralski (CZ) process for single-Si ingots is still very energy-intensive compared to the multi-crystalline ingot process [59].

Wafer thickness reduction has become one of the alternatives most adopted by various manufacturers, along with large wafers, to reduce production costs [61]. Wafer thickness varies according to the type of cell technology and wafer size. An average thickness of 170 µm has been observed for standard technology (p-type) and 130 µm for high-efficiency technology (n-type) in 2022. Thanks to the rapid cost reduction of mono-Si wafers and the aggressive capacity expansions carried out by the mono-wafers giants, mono-Si cells had reached over 95 % of market share by 2022 [18]. Characterized by improved performance and low cost, PERC technology has replaced the Al-BSF structure and became the dominant technology in the market in the 2020s. Module efficiency is a key parameter for manufacturers today. This has been greatly improved since 2014, from 16 % efficiency modules in 2014 to 20 % efficiency modules in 2021 [58]. Based on this benchmark, the BOM and performance of reference PV module is detailed in Table 2.

| | |
|---|---|
| **Polysilicon process** | Modified Siemens process |
| **Lingots type** | Mono-Si |
| **Wafer Thickness** | 170 µm |
| **Cell technology** | PERC |
| **Module power** | 326 Wp |
| **Frontsheet** | Glass (3.2 mm) |
| **Encapsulant** | EVA |
| **Backsheet** | PET |
| **Frame** | Aluminium |

*Table 2 Performance of the reference PV module*

More than 80 % of the production of the different components of the value chain of the PV module in 2022 is located in China. Therefore, we considered that all components (polysilicon, ingots, wafer, cells and modules) were produced in China for the evaluation of the reference module.

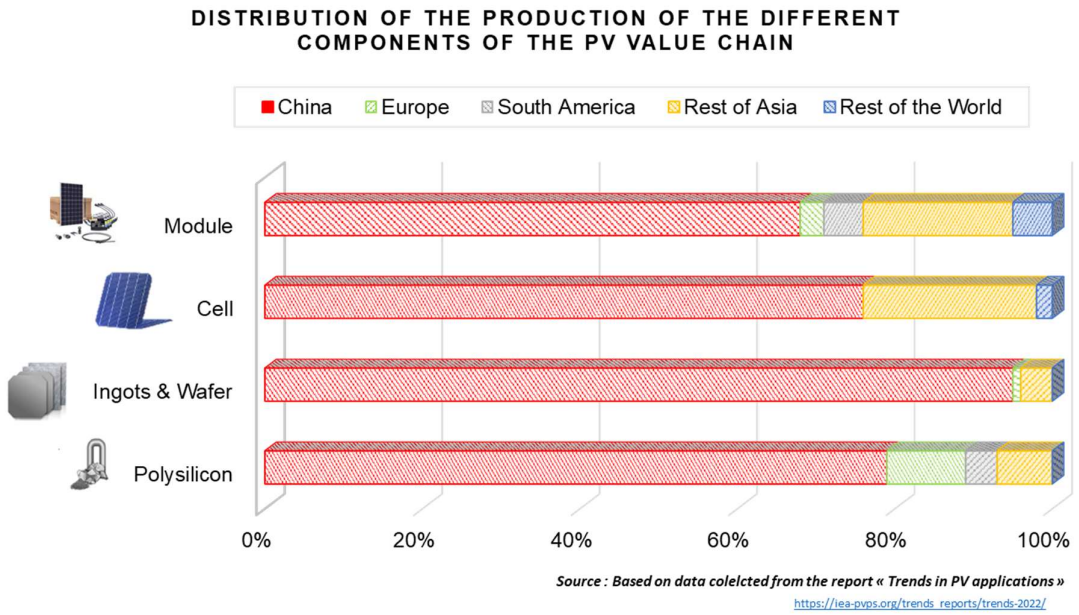


*Figure 1 : Distribution of the production of the different componenent of the PV value chain*

As a next step a life cycle inventory should be carried out. It is a flow analytical accounting estimating by quantifying the incoming and outgoing flows of energy and materials used during the entire life cycle of the product. The collected data must be representative of the current situation (good temporal, geographic and technological correlations). The data-collection is in accordance with the definition of objectives. All the data relative to the manufacturing stage of the PV module were collected from the internal database in CEA INES: materials (and their quantity) involved in the composition of the different layers of the structure, chemicals, water and energy consumption for the deposition process of the materials, emissions to air and water, and wastes.

## 3.2 Eco-design strategies

An LCA of reference was conducted for a standard PV module to identify the main steps to improve in order to reduce the environmental footprint of the PV module. This guided us to tackle the components with *the highest impact on the carbon footprint, namely the wafer, glass front sheet and aluminium frame.* The proposed improvements will be tested from technical point of view and economic point of view and the PV module will be developed.

The environmental footprint of the developed module will assess the sustainability.
Figure 2 illustrates the contribution of the different steps on the environmental impacts and therefore the bricks in the value chain to be eco-designed to make the PV panel green par excellence. The results show that:
- The production of polysilicon with Chinese energy mix, which is dominated by fossils energy, increases the carbon footprint impact
- The use of glass, ribbons, aluminium and silver has significant impacts on human health, resource depletion and ecosystem impacts.
- Copper consumption in ribbons has a significant impact on toxicity.
- Silver in cells has a significant impact on resource depletion.

The development of new technologies must therefore make it possible to reduce the consumption of these components or replace them, to ensure that these technologies are consistent with the eco-design approach.

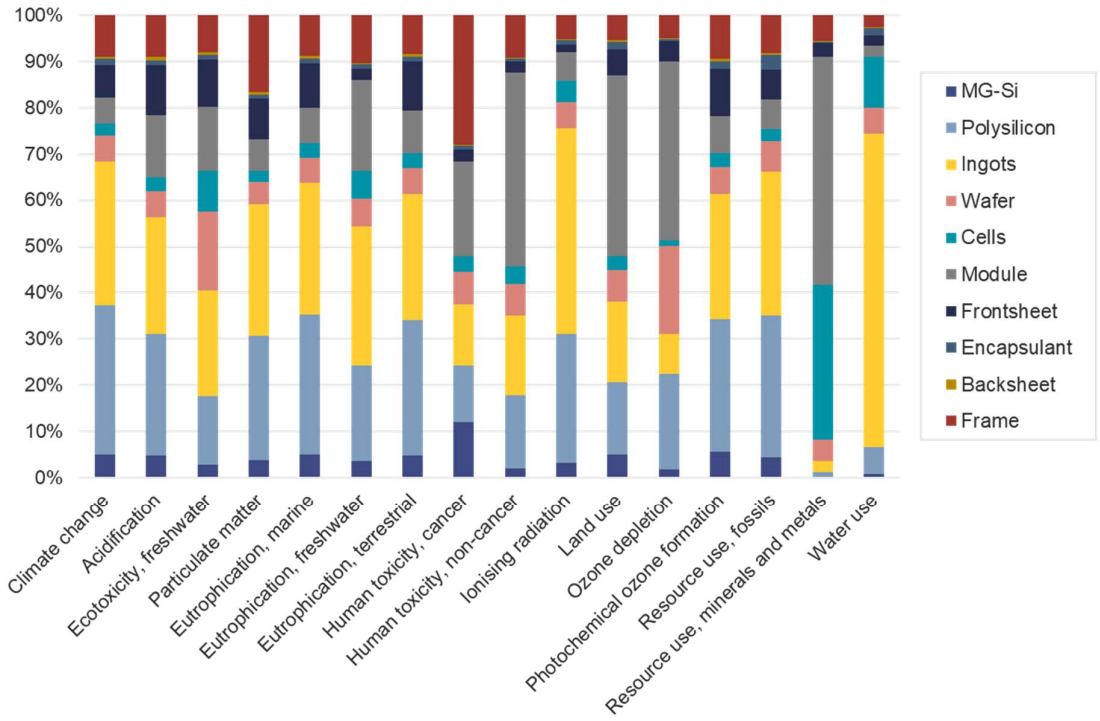


*Figure 2 Contribution of different steps to the environmental impacts*

## 3.3 Cell development

The solar cell contributes to the "Carbon footprint" criteria mainly via the silicon substrate used as a light absorber. Indeed, the production of this monocrystalline substrate implies the extraction, purification, and crystallization of ultra-pure silicon ingots, steps that require a large amount of energy. There are several means to reduce the "carbon footprint" of these wafers through, first, the *choice of production location.* Hence, we selected polysilicon from Germany and ingot produced in Norway, both countries having a low carbon electricity supply compared to China. Second, *reduction of the thickness of the wafers*, and thus the mass of silicon used (the relationship not being proportional) is an additional mean. Therefore, 130 µm as-cut wafers were used, while the standard thickness is in the range [160-180] µm. This choice does not imply any adjustment on our SHJ cells pilot line [62].

The heterojunction cells, with a rear emitter configuration and a metallization pattern with 6 busbars (BB) were prepared from M2 wafer format on the SHJ pilot line at CEA [63], [64]. The cells were manufactured in an eco-design approach with the objective of *reducing the consumption of critical materials: silver for the metallization, indium for the transparent conductive oxide* (TCO) [47] [34]. The average thickness of the finished cells is 115µm. The amount of TCO deposited on the backside of the cell has been reduced by 60 % (i.e., about 30 % reduction cell-wide) and each cell contains an average of 130 mg of silver paste. To

covert this value into an mg/W unite, we considered 92% of silver content in the paste (119.6 mg of Ag/cell). For a 22.5% cell yield, it represents approximately 21.7 mg of silver per watt. Optimizing the backside TCO is accompanied by an absolute 0.1% increase in efficiency (due to an increase in short-circuit current), while reducing the amount of silver paste is accompanied by a 0.25 % drop (due to a decrease in FF). The average performance of the cells was 22.5 % as presented in Figure 3. Table 3 presents global data on all produced solar cells.

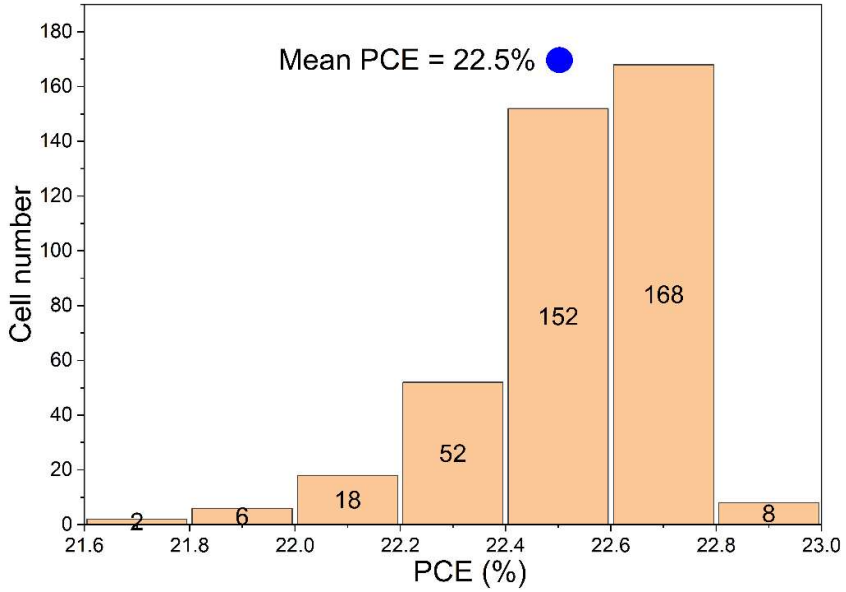


*Figure 3: Cell power conversion efficiency (PCE) distribution.*

| Data | N total | Mean | Standard Deviation | Minimum | Median | Maximum |
|---|---|---|---|---|---|---|
| $V_{oc}$ [mV] | 406 | 740.5 | 1.6 | 729.9 | 740.7 | 743.4 |
| $I_{sc}$ [A] | 406 | 9.26 | 0.02 | 9.21 | 9.26 | 9.32 |
| FF [%] | 406 | 80.31 | 0.64 | 77.13 | 80.46 | 81.35 |
| Eta [%] | 406 | 22.53 | 0.20 | 21.62 | 22.57 | **22.91** |
| RShunt [Ω] | 406 | 732 | 761 | 61 | 552 | 6700 |

*Table 3* Solar cell characteristics of the present study

## 3.4 Interconnection development

To guarantee a high module efficiency, which is also a critical lever in carbon footprint, the *gapless cell interconnection using ECA* (Electrically Conductive Adhesive) based gluing, and more specifically paving with -1mm cell-to cell offset has been selected. Paving is a module technology that enables PV cells to cover more of the module's surface in order to gain in power per unit area (Wp / m²). Similar to shingling, a variant of the paving technique also involves some overlapping of the cells. ECA-based interconnections have various advantages inherited from the family of adhesives such as a low toxicity (no lead), a tolerance toward mechanical deformation and a low processing temperature (between 120 °C and 200 °C compared to 250 °C for usual lead free solder). This latter property is

critical to reduce the thermo-mechanical stress enclosed in the wafer and makes this interconnection suitable for thin wafers [65].

The decrease of silver consumption during the cell interconnection processes is linked to the number of ribbons and the amount of ECA deposited on each cell busbar. To achieve economical sustainability, it is mandatory to find a method to reduce silver consumption. The first solution is to reduce the amount of ECA deposited on each BB. At the beginning of this optimization study, a straight solid line of ECA, 600 µm wide, was deposited on each BB. For a Half M2 cell, using a reference ECA, it represents about 5 mg of ECA per BB. To reduce the amount of silver we have depositing ECA pads instead of a continuous ECA line and use stencils screens to control perfectly the height and width of the ECA pads. These improvements have enabled deposited ECA's amount reduction by over 50% compared to the standard process. The challenge of the stringing part was thus to reconcile the paving technology with the thin cell thickness through process optimisation.

Paving interconnection requires adaptation of classical lamination process. As cell overlapping resulted inhomogeneous thickness increase everywhere in the module, it presents a risk of cell breakage during lamination. It can be handled by parameter (pressure, temperature, duration) adaptation and if required by adapting encapsulant thickness.

## 3.5 Module material selection

The glass-backsheet module configuration was selected to lower the environmental footprint with materials with proven reliability. Firstly, we selected a 2 mm thin glass enabling more than 30% of thickness reduction, which has a major impact on the carbon footprint.

Secondly, BOM with design for recycle and local sourcing approach motivated the choice of thermoplastic encapsulant and a fluorine-free backsheet. As presented in the introduction we opted for a TPO encapsulant from a European supplier. Generally, these encapsulants have a good optical performance (total light transmission rate over 90% on 280-1200nm light wavelength range) and a good adhesion strength may be obtained in a final PV module (>80 N/cm). Their melting temperature is higher (10°C over) than usual EVA encapsulants' thus the lamination process needs to be adapted. To maximise module performance, we selected from the same TPO in a transparent and a white variant behind solar cells owing to higher light reflection between the inter-string gaps and at module edges. This configuration enables up to 3 % of power gain. For the backsheet we selected a European manufacturer which propose a multi-layer backsheet with PET core layer without aluminium and without fluorine content.

As a first step of this part of the study, the encapsulant and backsheet has been characterized through a detailed material qualification sequence. This method has been presented earlier [66] and highlighting the importance of adhesion next to the WVTR level in backsheet selection to ensure reliability in damp heat testing conditions. Following these guidelines that a backsheet with the following adhesion of >40 N/cm and WVTR level of <2 g/m2/day has been selected. However, these datasheet values are valid for an EVA hence assessment of the TPO / backsheet interface with optimized lamination conditions is conducted following the methods described in section 2.3.

Peeling force remained over 50 N/cm even after 1000 h of DH exposure of the samples, confirming the compatibility of the materials. Afterwards reliability of the selected BOM with paving interconnection has been assessed on mini- modules through two sequences of IEC 61215-1:2021 standard. One module with its reference underwent the UV-TC- HF tests: 15 kWh of UV light exposure, 50cycles of thermal cycling and 10 cycles of humidity/freeze cycling. A second module and its reference underwent 1000h of damp heat (DH) exposure. Figure 4 shows no visible defect on the electroluminescence imaging, and

the test module had 6.7 % performance loss while the reference module had 12.3% after UV/TC/HF branch of the standard. DH testing were more severe for the selected BOM, and more important power losses had occurred. These losses were clearly due to the low moisture ingress resistance of the used encapsulant/BS material combination. Manufacturers had announced <2 g/m²/day for WVTR of the BS and 5 g/m²/day for WVTR of the TPO encapsulant in the datasheet respectively. Clearly, the combination of these two materials does not reach the required level of moisture resistance. In Figure 4 one can remark the difference between humidity ingress patterns. We can notice on the reference module darkening at gaps between cells. This is missing on the test module (left). It suggest that the overlapping cells in the string act as a moisture barrier by lengthening the moisture ingress path. This barrier is not present in the reference module, than moisture had entered between cells and caused darkening of the edges cells on the inter-cell zones ( which is correlated to loss of performance [68]).

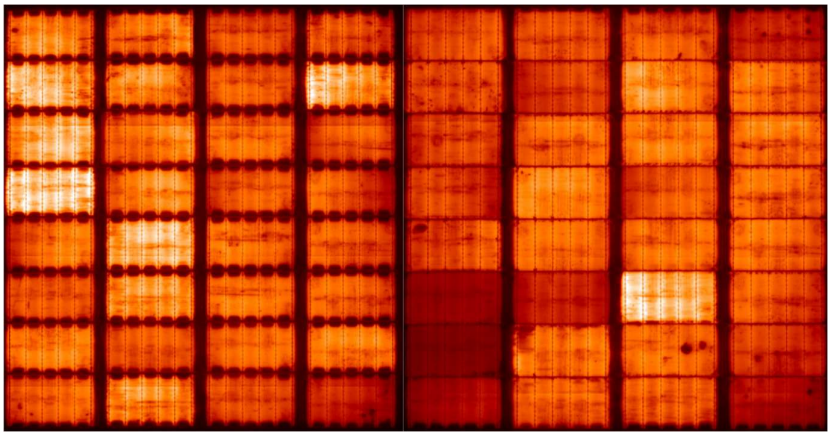

*Figure 4 Electroluminescence image of paving (left) and 2 mm inter-cell (right) modules after the branch UV/TC/HF of Standard 61215-1[53] (without DML)*

Maintaining the durability of PV modules is critical to ensure their low environmental impact, and with the constraint of non-toxic materials, local sourcing that as intermediate solution we still retained a combination of TPO and PET/Al/PET multi-layer backsheet stack proven to limit the module degradation [30], [31]. To further reduce the environmental impact of the BOM two possibilities are identified with either a non-fluorine, non-aluminised backsheet or TPO encapsulant with lower water vapour transmission rate (WVTR). To replace this performance a careful combination of encapsulant and backsheet should be selected to counterbalance the lack of impermeable Al layer [66].

### 3.5.1 Frame design: case study of wooden frames

Following eco-design approach, aluminium has the second highest impact on the carbon footprint hence its replacement with low bio-carbon alternative was a critical step. As a case study of novel type of frame qualification, we conducted both material level coupled ageing and mechanical testing as well as module level indoor and outdoor testing.

For this case study, we present the replacement of aluminium framing by a timber frame. Plant-based/bio-sourced materials are a promising avenue under investigation for certain segment of PV application. This replacement required a frame section development as wood has lower mechanical strength than aluminium. The wooden frame, selected as a first case study of the methodology, is novel material family hence an initial selection has been conducted based on the quality, hardness, weather resistance of various wooden types.

To be able to serve as a frame for a PV module, the wood's most important characteristics are the mechanical strength, the durability, fire resistance needs to last as long as the rest of the module and maintaining the overall structure. Additionally, low maintenance was as also considered in the selection. Wood frame design recommendations suggest the durability sorts 3b and 4 according to French standard [69] which correspond to outdoor use, without ground contact and with exposure to weathering. The list of chosen wood species and their durability sorting are listed in Table 4.
Five wood species were targeted: the acacia, the oak, the chestnut, the spuce and a tropical species the opepe (bilinga). The chosen species are all without maintenance and no need of treatments during service life.

| Species | Acacia | Oak | Chestnut | Spuce | Opepe (Bilinga) |
|---|---|---|---|---|---|
| Durability | 4 | 3b | 3b | 3b | 4 |

*Table 4 Durability sorting of studied wood species, according to national standards and design recommendations[70]*

We used three methods for the dimensioning of the wood frame, namely Eurocode EC5 [71], National standard method (implemented into a software); Finite element method (FEM) in SolidWorks. The first method enables to assess security coefficients, the maximum charges on structure; the second method gives the sections of the structure while the third one enables to study the complete module's behaviour with its timber frame under previously determined maximum charges. The detailed mechanical study of the frame is out of scope of this paper.

Mechanical properties of the selected species, namely, the Young modulus and tensile stress have been extracted from four-point bending tests [56] conducted on frame elements before and after accelerated ageing tests (thermal cycling and humidity freeze tests) as shown in *Table 5*.

| Frame material | Flexural strength (MPa) | | | Young modulus (GPa) | | |
|---|---|---|---|---|---|---|
| | **Initial stage** | **After TC** | **After HF** | **Initial stage** | **After TC** | **After HF** |
| Aluminium | 62 | - | - | 46.3 | - | - |
| Acacia | 120±18 | 130±3 | 120±29 | 22±0,8 | 21±1,2 | 21±1,2 |
| Chestnut | 120±6 | 110±22 | 100±14 | 21±1 | 19±0,8 | 27±1,4 |
| Oak | 110±5 | 140±0 | 110±13 | 17±1,8 | 22±0 | 23±3,8 |
| Opope (Bilinga) | 100±32 | 80±25 | 80±35 | 20±3 | 16±4,3 | 19±4,9 |
| Spurce | 70±12 | 80±34 | 60±11 | 19±0,6 | 19±4,5 | 18±4,6 |

*Table 5 Reference aluminium and studied wood species' four point bending rupture strength and Young modulus at initial stage, after TC and HF ageing*

We expected flexural strength and Young modulus decrease after aging which was the case only for chestnut and bilinga for flexural strength that decreased of 10-20 MPa upon aging while acacia or oak does not suffer from this same effect. We can highlight that Young modulus was nearly not affected by aging except for bilinga which lost 4 GPa after thermal cycling. After this testing sequence all the preselected wood species were validated for frame integration. The wood transformation required several steps before obtaining the finalised wood frame.

Finally, assembly of full sized PV modules with the different species to evaluate their load resistance through two ageing sequence. We submitted the first group to static mechanical loading (SML) test at 5400 Pa following IEC61215 before and after 200 thermal cycles between -40 °C-85 °C. Second group of the modules was tested in SML after 10 cycles of humidity freeze. Several species showed an increase in deflection of more than 200% compared with aluminium, which generated failure, frame cracking in the test. Following the combined material and module level qualification, acacia has been selected as frame material. In addition, this wood species is widely available in Europe. We can conclude that the manufacture of PV modules with natural fibre could be relevant for certain applications. However, estimates of total lifetime cannot be made at this stage, which is why the different module variants are being aged outdoors to gain a better understanding of the durability of assemblies, which can have an impact on frame stability. Future optimization should focus on frame assembly techniques to ensure high resistance to weather-induced degradation. In addition, a comprehensive qualification process will have to be carried out to determine the extended performance of wood frames compared with aluminium frames. This work aims to pave the way towards exploration of novel material types for framing to ensure a massive reduction of environmental footprint of PV modules.

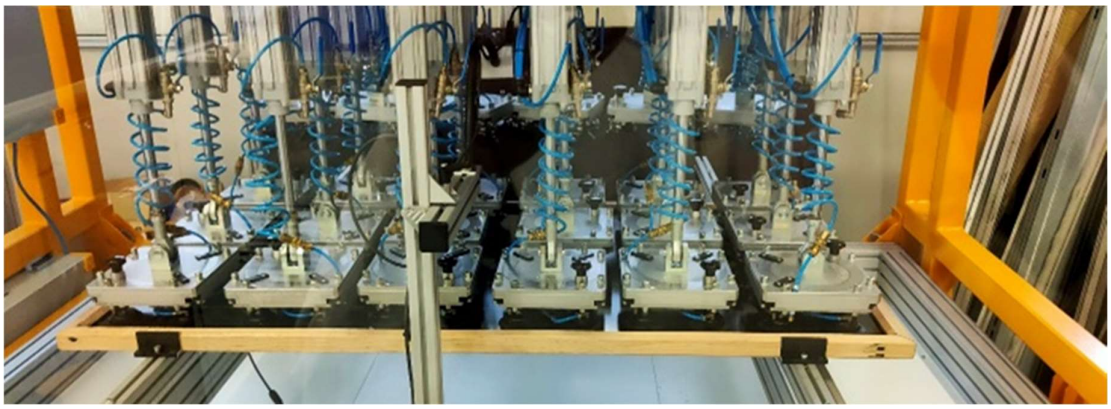

*Figure 5 SML/DML test bench at our laboratory with timber framed PV module under testing*

Figure 6 presents the final, full size PV module obtained with all combined technologies presented in this study framed with acacia.

*Figure 6 Photography of finalised framed module (without ageing)*

## 3.6 Final LCA analysis of the module

Finally the proof of concept module demonstrator of 566 Wp combining the cells module technologies and materials presented in the previous sections.
Complete LCA of the prototype PV module was conducted based on the selected materials, and tehcnologies. As details in Figure 7, results shows a significant reduction of the carbon footprint compared to the reference presented in section 2. The carbon footprint of the module developed is equal to 317 kgCO2eq/kWp, thus considered a very low-carbon PV panel compared to standard Chinese panels whose value today varies between 700 and 800 kgCO2eq / kWp. The carbon footprint of this module is also considered a forefront in among other pioneering modules for example by REC (411 $kgCO_2eq$ / kWp) [72], Bisol (411 $kgCO_2eq$ / kWp) [73], Qcells (386 $kgCO_2eq$ / kWp) JinkoSolar (450 $kgCO_2eq$ / kWp) [74], Trina Solar (386 $kgCO_2eq$ /kWp) [75], Husan (366.12 $kgCO_2eq$ /kWp) [76] without being exhaustive. This low carbon footprint is mainly due to the module's production location between Germany, Norway and France. These countries are characterized by very low-carbon electricity mixes estimated at 635 gCO2eq / kWh, 29 gCO2eq / kWh and 52 gCO2eq / kWh, compared with a Chinese mix whose carbon footprint is equal to 1024 gCO2eq / kWh [77]. The thickness of the glass and wafer also reduces the carbon footprint. Replacing the aluminum frame with a timber frame reduced the carbon footprint by more than 50-60 kgCO2eq / kWp (Figure 7). The timber frame has other benefits of the reduction of risks to human health (20%) and the depletion of fossil resources (50%).Therefore, by optimizing technical parameters and selecting environmental-friendly materials, we were able to develop an eco-designed PV module with a very low carbon footprint.

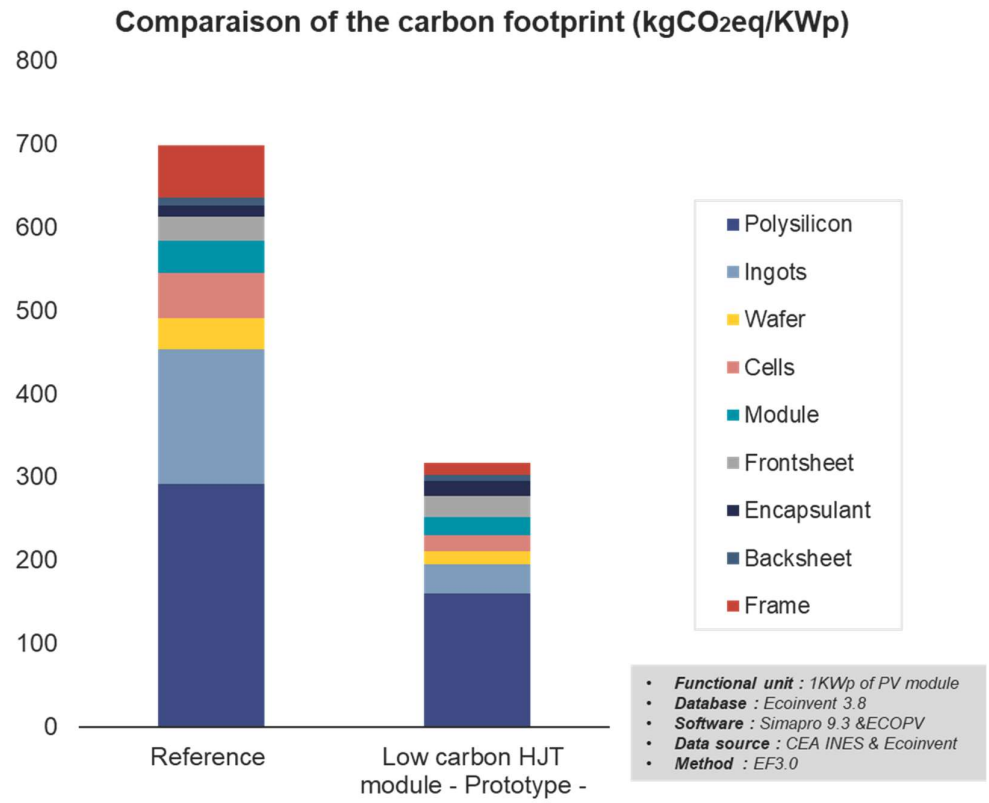


*Figure 7 Comparison of carbon footprint of standard module (left) and ultra low carbon SHJ module prototype developed in this study (right)*

# 4 Conclusion

In this study, we presented a module design driven by LCA sensitivity analysis to reach ultra-low carbon impact PV module with outstanding performance. A preliminary LCA analysis of standard PV module suggested three highest impact materials to lower considerably its environmental impact:

- silicon wafer,
- aluminium frame and
- front glass.

Carbon footprint reduction on cell level focused on the reduction of the wafer thickness combined with sourcing from production site with low carbon electricity supply, in this study polysilicon, ingot and wafer issued from the European value chain. Paving interconnection and new cell metallization enabled decreasing silver consumption. At the module level, the reduction of glass thickness and the replacement of the aluminum frame with a low carbon frame have been selected in a glass-backsheet module configuration. In addition, a "design for recycle" approach was implemented for the choice of encapsulant and backsheet retaining a thermoplastic material and multi-layer PET backsheet. We presented the integration and qualification tests of the different elements of the BOM. The combination of these innovations led us to the realization of a 566 Wp module based on a GapLess interconnection with single heterojunction cells of average efficiency of 22.6% with a carbon footprint of 317 $kgCO_2eq/kWp$.

Nevertheless, our study showed the importance of finding a compromise between environmental impact optimization and module performance and durability. Specifically, to maintaining durability required to select multi-layer backsheet with aluminum core layer despite its higher impact compared to full polymer backsheets. For this reason to further lower module's environmental impact, alternative backsheet materials without aluminum and fluorine are under investigation. Similarly, the wooden frame is case study for qualification of alternative material for framing however, its reliability is not fully proven, but it remains adapted to some PV applications.
Future innovations are aimed at the same time at the performance increase and important reduction of the In and Ag consumption both at cell and module level as well as integration of recycled material content at all stages of the value chain to ensure a sustainable TerraWatt scale deployment of PV.

# 5 Acknowledgement

The authors acknowledge INES2S, ITE for the financial support of this study.

# 6 REFERENCES

[1] S. Dale, « Statistical Review of World Energy 2022 », 2022.
[2] « NEW! Report on Eco-design & Energy Labelling for PV modules, inverters and systems in the EU - Other news - ETIP PV ». Consulté le: 26 juin 2023. [En ligne]. Disponible sur: https://etip-pv.eu/news/other-news/new-report-on-eco-design-energy-labelling-for-pv-modules-inverters-and-systems-in-the-eu/
[3] « La CRE publie les cahiers des charges des nouvelles périodes des appels d'offres dit "PPE2 Eolien", "PPE2 PV Bâtiment" et "PPE2 PV Sol" et accompagne les porteurs de projets ». Consulté le: 19 juin 2023. [En ligne]. Disponible sur: https://www.cre.fr/Actualites/la-cre-publie-les-cahiers-des-charges-des-nouvelles-periodes-des-appels-d-offres-dit-ppe2-eolien-ppe2-pv-batiment-et-ppe2-pv-sol-et-accompag
[4] « EPEAT Registry ». Consulté le: 26 juin 2023. [En ligne]. Disponible sur: https://www.epeat.net/
[5] lds2015, « Le panneau solaire REC Alpha Pure sans plomb obtient la certification CERTISOLIS bas carbone », L'Echo du Solaire. Consulté le: 26 juin 2023. [En ligne]. Disponible sur: https://www.lechodusolaire.fr/le-panneau-solaire-rec-alpha-pure-sans-plomb-obtient-la-certification-certisolis-bas-carbone/
[6] « Q CELLS' Q.PEAK DUO modules earn further low-carbon certification for French tenders - Q CELLS South East Asia ». Consulté le: 26 juin 2023. [En ligne]. Disponible sur: http://qcells.com/ane/stay-in-the-loop/trending-news-detail?newsId=NEW220126154652050
[7] « Aspect environnemental ». Consulté le: 26 juin 2023. [En ligne]. Disponible sur: https://www.voltec-solar.com/Fr/Societe/Aspect-environnemental.html
[8] P. K. Singh et P. Sarkar, « Eco-design Approaches for Developing Eco-friendly Products: A Review », in *Advances in Industrial and Production Engineering*, K. Shanker, R. Shankar, et R. Sindhwani, Éd., in Lecture Notes in Mechanical Engineering. Singapore: Springer, 2019, p. 185-192. doi: 10.1007/978-981-13-6412-9_17.
[9] « Life Cycle Assessment Methodology - an overview | ScienceDirect Topics ». Consulté le: 26 juin 2023. [En ligne]. Disponible sur: https://www.sciencedirect.com/topics/engineering/life-cycle-assessment-methodology
[10] « NF EN ISO 14040:2016 Management environnemental - Analyse du cycle de vie - Principes et cadre », févr. 2021. Consulté le: 2 février 2021. [En ligne]. Disponible sur:

https://sagaweb.afnor.org/fr-FR/splus/consultation/notice/1279520?recordfromsearch=True
[11] « NF EN ISO 14040/A1:2020 Management environnemental - Analyse du cycle de vie - Principes et cadre - Amendement 1 ».
[12] « NF EN ISO 14044 COMPIL 1 Management environnemental - Analyse du cycle de vie - Exigences et lignes directrices - Texte compilé de la norme NF EN ISO 14044 d'octobre 2006 et de son amendement A1 de février 2018 », NORME NF EN ISO 14044 COMPIL 1, févr. 2018. Consulté le: 19 janvier 2021. [En ligne]. Disponible sur: https://sagaweb.afnor.org/fr-FR/splus/consultation/notice/1532755?recordfromsearch=True
[13] N. Gazbour, « Intégration systémique de l'éco-conception dès la phase de R&D des technologies photovoltaïques », phdthesis, Université Grenoble Alpes, 2019. Consulté le: 21 juin 2023. [En ligne]. Disponible sur: https://theses.hal.science/tel-02373608
[14] N. Gazbour *et al.*, « A path to reduce variability of the environmental footprint results of photovoltaic systems », *J. Clean. Prod.*, vol. 197, p. 1607-1618, oct. 2018, doi: 10.1016/j.jclepro.2018.06.276.
[15] V. Muteri *et al.*, « Review on Life Cycle Assessment of Solar Photovoltaic Panels », *Energies*, vol. 13, nº 1, Art. nº 1, janv. 2020, doi: 10.3390/en13010252.
[16] Z. Liu *et al.*, « Revisiting thin silicon for photovoltaics: a technoeconomic perspective », *Energy Environ. Sci.*, vol. 13, nº 1, p. 12-23, 2020, doi: 10.1039/C9EE02452B.
[17] X. Jia, C. Zhou, Y. Tang, et W. Wang, « Life cycle assessment on PERC solar modules », *Sol. Energy Mater. Sol. Cells*, vol. 227, p. 111112, août 2021, doi: 10.1016/j.solmat.2021.111112.
[18] A. Müller, L. Friedrich, C. Reichel, S. Herceg, M. Mittag, et D. H. Neuhaus, « A comparative life cycle assessment of silicon PV modules: Impact of module design, manufacturing location and inventory », *Sol. Energy Mater. Sol. Cells*, vol. 230, p. 111277, sept. 2021, doi: 10.1016/j.solmat.2021.111277.
[19] A. Singh, V. Umakanth, N. Tyagi, et S. Kumar, « A comparative study of different polymer materials for the development of flexible crystalline silicon modules », *Sol. Energy Mater. Sol. Cells*, vol. 255, p. 112259, juin 2023, doi: 10.1016/j.solmat.2023.112259.
[20] Chr. Lamnatou, A. Moreno, D. Chemisana, F. Reitsma, et F. Clariá, « Ethylene tetrafluoroethylene (ETFE) material: Critical issues and applications with emphasis on buildings », *Renew. Sustain. Energy Rev.*, vol. 82, p. 2186-2201, févr. 2018, doi: 10.1016/j.rser.2017.08.072.
[21] J. F. Bouquet, « Glass for Low-Cost Photovoltaic Solar Arrays ». 1 février 1980.
[22] B. L. Allsopp *et al.*, « Towards improved cover glasses for photovoltaic devices », *Prog. Photovolt. Res. Appl.*, vol. 28, nº 11, p. 1187-1206, 2020, doi: 10.1002/pip.3334.
[23] G. Oreski *et al.*, « Designing New Materials for Photovoltaics: Opportunities for Lowering Cost and Increasing Performance through Advanced Material Innovations », SAND--2021-4837R, 1779380, 695676, avr. 2021. doi: 10.2172/1779380.
[24] M. Vite *et al.*, « Improving the Reliability of a Solar Road PV Module », *37th Eur. Photovolt. Sol. Energy Conf. Exhib. 1706-1710*, p. 5 pages, 4873 kb, 2020, doi: 10.4229/EUPVSEC20202020-6DO.11.4.
[25] B. Adothu, F. R. Costa, et S. Mallick, « Damp heat resilient thermoplastic polyolefin encapsulant for photovoltaic module encapsulation », *Sol. Energy Mater. Sol. Cells*, vol. 224, p. 111024, juin 2021, doi: 10.1016/j.solmat.2021.111024.
[26] H. A. A. Mahdi, P. G. Leahy, et A. P. Morrison, « Predicting Early EVA Degradation in Photovoltaic Modules From Short Circuit Current Measurements », *IEEE J.*

*Photovolt.*, vol. 11, nº 5, p. 1188-1196, sept. 2021, doi: 10.1109/JPHOTOV.2021.3086455.
[27] M. C. C. de Oliveira, A. S. A. Diniz Cardoso, M. M. Viana, et V. de F. C. Lins, « The causes and effects of degradation of encapsulant ethylene vinyl acetate copolymer (EVA) in crystalline silicon photovoltaic modules: A review », *Renew. Sustain. Energy Rev.*, vol. 81, p. 2299-2317, janv. 2018, doi: 10.1016/j.rser.2017.06.039.
[28] O. K. Segbefia, A. G. Imenes, et T. O. Sætre, « Moisture ingress in photovoltaic modules: A review », *Sol. Energy*, vol. 224, p. 889-906, août 2021, doi: 10.1016/j.solener.2021.06.055.
[29] P. Danz, V. Aryan, E. Möhle, et N. Nowara, « Experimental Study on Fluorine Release from Photovoltaic Backsheet Materials Containing PVF and PVDF during Pyrolysis and Incineration in a Technical Lab-Scale Reactor at Various Temperatures », *Toxics*, vol. 7, nº 3, p. 47, sept. 2019, doi: 10.3390/toxics7030047.
[30] Y. Zhang, M. Kim, L. Wang, P. Verlinden, et B. Hallam, « Design considerations for multi-terawatt scale manufacturing of existing and future photovoltaic technologies: challenges and opportunities related to silver, indium and bismuth consumption », *Energy Environ. Sci.*, vol. 14, nº 11, p. 5587-5610, nov. 2021, doi: 10.1039/D1EE01814K.
[31] B. Hallam *et al.*, « The silver learning curve for photovoltaics and projected silver demand for net-zero emissions by 2050 », *Prog. Photovolt. Res. Appl.*, vol. 31, nº 6, p. 598-606, 2023, doi: 10.1002/pip.3661.
[32] A. Valero, A. Valero, G. Calvo, et A. Ortego, « Material bottlenecks in the future development of green technologies », *Renew. Sustain. Energy Rev.*, vol. 93, p. 178-200, oct. 2018, doi: 10.1016/j.rser.2018.05.041.
[33] « Resilex – Resilient Enhancement for the Silicon Industry Leveraging the European Matrix ». Consulté le: 1 août 2023. [En ligne]. Disponible sur: https://www.resilex-project.eu/
[34] T. Gageot *et al.*, « Feasibility test of drastic indium cut down in SHJ solar cells and modules using ultra-thin ITO layers », *Sol. Energy Mater. Sol. Cells*, vol. 261, p. 112512, oct. 2023, doi: 10.1016/j.solmat.2023.112512.
[35] « Photorama ». Consulté le: 1 août 2023. [En ligne]. Disponible sur: https://www.photorama-project.eu/
[36] « Steel Module Frames | Origami Solar, Inc. » Consulté le: 11 septembre 2023. [En ligne]. Disponible sur: https://origamisolar.com/steel-solar-module-frames/
[37] K. Pickerel, « Steel is being considered as an alternative to aluminum solar panel frames », Solar Power World. Consulté le: 11 septembre 2023. [En ligne]. Disponible sur: https://www.solarpowerworldonline.com/2022/08/steel-is-seriously-being-considered-as-an-alternative-to-aluminum-solar-panel-frames/
[38] A. Bhambhani, « Risen Energy's Steel Frame HJT Module In Mass Production », TaiyangNews. Consulté le: 11 septembre 2023. [En ligne]. Disponible sur: https://taiyangnews.info/technology/risen-energys-steel-frame-hjt-module-in-mass-production/
[39] « LG Chem in Everyday Life | PR Center | Company | LG Chem ». Consulté le: 11 septembre 2023. [En ligne]. Disponible sur: https://www.lgchem.com/company/information-center/life-in-lgchem/life-in-lgchem-detail-4690
[40] A. Tummalieh, A. J. Beinert, C. Reichel, M. Mittag, et H. Neuhaus, « Holistic design improvement of the PV module frame: Mechanical, optoelectrical, cost, and life cycle analysis », *Prog. Photovolt. Res. Appl.*, vol. 30, nº 8, p. 1012-1022, 2022, doi: 10.1002/pip.3533.

[41] T. Singer, « Wooden Photovoltaic Module Frames: Proof of Concept, Life Cycle Assessment and Cost Analysis », Master Thesis, Uppsala University, Uppsala, 2021. [En ligne]. Disponible sur: https://www.diva-portal.org/smash/get/diva2:1597901/FULLTEXT01.pdf

[42] M. F. T. Hossain, S. Dessouky, A. B. Biten, A. Montoya, et D. Fernandez, « Harvesting Solar Energy from Asphalt Pavement », *Sustainability*, vol. 13, nº 22, Art. nº 22, janv. 2021, doi: 10.3390/su132212807.

[43] N. Vandewetering, K. S. Hayibo, et J. M. Pearce, « Impacts of Location on Designs and Economics of DIY Low-Cost Fixed-Tilt Open Source Wood Solar Photovoltaic Racking », *Designs*, vol. 6, nº 3, Art. nº 3, juin 2022, doi: 10.3390/designs6030041.

[44] E. S. Mazzucchelli, M. Alston, M. Brzezicki, et L. Doniacovo, « Study of a BIPV Adaptive System: Combining Timber and Photovoltaic Technologies », *J. Facade Des. Eng.*, vol. 6, nº 3, p. 149-162, nov. 2018, doi: 10.7480/jfde.2018.3.2602.

[45] K. Farkas *et al.*, « Designing Photovoltaic Systems for Architectural Integration », IEA Solar Heating and Cooling Programme, nov. 2013. doi: 10.18777/ieashc-task41-2013-0002.

[46] F. Vallet, B. Eynard, D. Millet, S. G. Mahut, B. Tyl, et G. Bertoluci, « Using eco-design tools: An overview of experts' practices », *Des. Stud.*, vol. 34, nº 3, p. 345-377, mai 2013, doi: 10.1016/j.destud.2012.10.001.

[47] F. Jay *et al.*, « Reduction in Indium Usage for Silicon Heterojunction Solar Cells in a Short-Term Industrial Perspective », *Sol. RRL*, vol. 7, nº 8, p. 2200598, 2023, doi: 10.1002/solr.202200598.

[48] L. Basset, W. Favre, D. Muñoz, et J.-P. Vilcot, « Series Resistance Breakdown of Silicon Heterojunction Solar Cells Produced on CEA-INES Pilot Line », in *35th European Photovoltaic Solar Energy Conference and Exhibition; 721-724*, WIP, 2018, p. 4 pages, 6926 kb. doi: 10.4229/35THEUPVSEC20182018-2DV.3.21.

[49] W. Favre *et al.*, « 25% Efficient Large Area Silicon Solar Cell: Paving the Way for Premium PV Manufacturing in Europe », présenté à EU PVSEC 2020, in 2BO.5.7. on-line, 11/9 2020.

[50] D. Muñoz, « Heterojunction solar cells: reducing the gap from lab to fab », présenté à 3rd Int. Workshop on Silicon Heterojunction Solar Cells, on-line, 21/10 2020.

[51] N. Bassi *et al.*, « GridTOUCH: Innovative Solution for Accurate IV Measurement of Busbarless Cells in Production and Laboratory Environments », in *29th European Photovoltaic Solar Energy Conference and Exhibition; 1180-1185*, WIP, 2014, p. 6 pages, 16194 kb. doi: 10.4229/EUPVSEC20142014-2BV.8.24.

[52] R. Monna *et al.*, « Latest advances of ECA-based tabbing and stringing at CEA-INES », *PHOTOVOLTAICS INTERNATIONAL*, vol. Edition 48, 22 juin 2022. Consulté le: 28 juillet 2023. [En ligne]. Disponible sur: https://www.pv-tech.org/technical-papers/latest-advances-of-eca-based-tabbing-and-stringing-at-cea-ines/

[53] « EN IEC 61215-1:2021: Terrestrial photovoltaic (PV) modules - Design qualification and type approval - Part 1 : test requirements ». Consulté le: 13 avril 2023. [En ligne]. Disponible sur: https://www.boutique.afnor.org/fr-fr/norme/nf-en-iec-612151/modules-photovoltaiques-pv-pour-applications-terrestres-qualification-de-la/fa195378/238021

[54] « IEC 62788-1-6:2017: Measurement procedures for materials used in photovoltaic modules - Part 1-6: Encapsulants - Test methods for determining the degree of cure in Ethylene-Vinyl Acetate ». 2017. Consulté le: 17 juillet 2023. [En ligne]. Disponible sur: https://webstore.iec.ch/publication/33050

[55] « ISO 3133:1975: Wood — Determination of ultimate strength in static bending ». Consulté le: 27 septembre 2023. [En ligne]. Disponible sur: https://www.iso.org/standard/8291.html
[56] « ASTM D6272-17e1: Standard Test Method for Flexural Properties of Unreinforced and Reinforced Plastics and Electrical Insulating Materials by Four-Point Bending ». Consulté le: 26 septembre 2023. [En ligne]. Disponible sur: https://www.astm.org/d6272-17e01.html
[57] « IEC TS 62782:2016 Photovoltaic (PV) modules - Cyclic (dynamic) mechanical load testing ». Consulté le: 26 septembre 2023. [En ligne]. Disponible sur: https://webstore.iec.ch/publication/24310
[58] « International Technology Roadmap for Photovoltaic (ITRPV) - vdma.org - VDMA ». Consulté le: 19 juin 2023. [En ligne]. Disponible sur: https://www.vdma.org/international-technology-roadmap-photovoltaic
[59] « Trends in PV Applications 2022 », IEA-PVPS. Consulté le: 26 juin 2023. [En ligne]. Disponible sur: https://iea-pvps.org/trends_reports/trends-2022/
[60] M. Gueydan, « Solaire photovoltaïque : quel impact sur l'environnement ? », Encyclopédie de l'énergie. Consulté le: 21 juin 2023. [En ligne]. Disponible sur: https://www.encyclopedie-energie.org/solaire-photovoltaique-impact-environnement/
[61] « TOP SOLAR MODULES H1/2023 | TaiyangNews ». Consulté le: 26 juin 2023. [En ligne]. Disponible sur: https://taiyangnews.info/reports/top-solar-modules-h1-2023/
[62] S. Dubois *et al.*, « n-type silicon solar cells », in *n-Type Crystalline Silicon Photovoltaics: Technology, applications and economics*, IET Digital Library, 2022, p. 69-170. doi: 10.1049/PBPO175E_ch3.
[63] F. Pernoud *et al.*, « Recent developments of HJT screen printing process at CEA-INES with silver paste », in *MIW Metallization and Interconnection Workshop*, Neuchatel, Swiss, mai 2023. Consulté le: 28 juillet 2023. [En ligne]. Disponible sur: https://miworkshop.info/wp-content/uploads/2023/05/P1_-MIW23_Recent-developments-of-HJT-screen-printing-process-at-CEA-INES-.pdf
[64] A. Danel *et al.*, « Versatile Pilot Line to Support the Heterojunction Solar Cell Industrial Development: Busbar and Busbar-Less Configurations », *33rd Eur. Photovolt. Sol. Energy Conf. Exhib. 447-450*, p. 4 pages, 2801 kb, 2017, doi: 10.4229/EUPVSEC20172017-2DO.1.5.
[65] V. Barth *et al.*, « Electrically Conductive Adhesive industrial strategy approach for HJT solar cells », présenté à Metallization and Interconnection Workshop MIW, Genk, Belgium, nov. 2021. [En ligne]. Disponible sur: https://miworkshop.info/presentations-2021/
[66] T. Bejat *et al.*, « Extensive Module Backsheet Qualification Protocol Correlated to SHJ Module Reliability », in *8th World Conference on Photovoltaic Energy Conversion*, WIP, déc. 2022, p. 577-579. doi: 10.4229/WCPEC-82022-3DO.17.3.
[67] T. Bejat *et al.*, « Design for the Environment: HJT Module with Ultra-Low Carbon Footprint », présenté à 40th EU PVSEC 2023, Lisbon, Portugal, 21 septembre 2023. [En ligne]. Disponible sur: www.eupvsec.org
[68] T. H. Kim, N. C. Park, et D. H. Kim, « The effect of moisture on the degradation mechanism of multi-crystalline silicon photovoltaic module », *Microelectron. Reliab.*, vol. 53, nº 9, p. 1823-1827, sept. 2013, doi: 10.1016/j.microrel.2013.07.047.
[69] « Fascicule de documentation FD P20-651 ». AFNOR, juillet 2011. Consulté le: 4 août 2023. [En ligne]. Disponible sur: https://www.boutique.afnor.org/fr-fr/norme/fd-p20651/durabilite-des-elements-et-ouvrages-en-bois/fa174309/37584
[70] « NF DTU 59.1: Travaux de bâtiment - Revêtements de peinture en feuil mince, semi-épais, ou épais - Partie 1-2 : critères généraux de choix des matériaux ». Consulté

le: 26 septembre 2023. [En ligne]. Disponible sur: https://www.boutique.afnor.org/fr-fr/norme/nf-dtu-591/travaux-de-batiment-revetements-de-peinture-en-feuil-mince-semiepais-ou-epa/fa183018/1371

[71] « BS EN 1995-1-1:2004+A2:2014 Eurocode 5: Design of timber structures General. Common rules and rules for buildings - European Standards ». 1995. Consulté le: 4 août 2023. [En ligne]. Disponible sur: https://www.en-standard.eu/bs-en-1995-1-1-2004-a2-2014-eurocode-5-design-of-timber-structures-general-common-rules-and-rules-for-buildings/

[72] « Another green check for the lead-free1 REC Alpha Pure: Certified as a Low Carbon Footprint solar panel », REC Group. Consulté le: 19 juin 2023. [En ligne]. Disponible sur: https://www.recgroup.com/en/news/another-green-check-lead-free1-rec-alpha-pure-certified-low-carbon-footprint-solar-panel

[73] « Solar Products | Certificates », BISOL. Consulté le: 19 juin 2023. [En ligne]. Disponible sur: https://www.bisol.com/certificates

[74] « JinkoSolar: - France: Tiger Neo Bifacial modules certified for low carbon footprint ». Consulté le: 19 juin 2023. [En ligne]. Disponible sur: https://www.pveurope.eu/solar-modules/jinkosolar-france-tiger-neo-bifacial-modules-certified-low-carbon-footprint

[75] « FR/New Trina Solar Vertex N modules redefine high-efficiency products, 10GW+ capacity to be released in the first quarter of 2023 », Trina Solar. Consulté le: 31 août 2023. [En ligne]. Disponible sur: https://www.trinasolar.com/fr/resources/newsroom/wed-10192022-1530

[76] « 366.12g/W $CO_2e$ ! Huasun Released Carbon Footprint Report Certified by TÜV Rheinland! », Anhui Huasun Energy Co., Ltd. Consulté le: 31 août 2023. [En ligne]. Disponible sur: https://www.huasunsolar.com/366.12g-w-co2e-huasun-released-carbon-footprint-report-certified-by-tuv-rheinland.html

[77] « ecoinvent Database - ecoinvent ». Consulté le: 26 juin 2023. [En ligne]. Disponible sur: https://ecoinvent.org/the-ecoinvent-database/